Journal of Associated Medical Sciences 2024; 57(2): 141-148

JAMS
Journal of Associated Medical Sciences

Scopus Indexed & Thai-Journal Citation Index Centre (TCI)

Journal of Associated Medical Sciences

Journal homepage: https://www.tci-thaijo.org/index.php/bulletinAMS/index

Evaluation of the offset couch parameter between kilovoltage on-board imaging and cone-beam computed tomography in patients with prostate cancer

Tanaporn Guawgumnerdtong[1,2] Nuanpen Damrongkijudom[3] Achawee Suwanarat[3] Piyawan Chailapakul[2] Tawatchai Ekjeen[3*]

[1]Master of Science in Radiological Technology Programme, Faculty of Medical Technology, Mahidol University, Nakhon Pathom Province, Thailand.
[2]Department of Radiation Oncology, Chulabhorn Hospital, Chulabhorn Royal Academy, Bangkok, Thailand.
[3]Department of Radiological Technology, Faculty of Medical Technology, Mahidol University, Nakhon Pathom Province, Thailand.

ARTICLE INFO

Article history:
Received 25 October 2023
Accepted as revised 18 March 2024
Available online 21 March 2024

Keywords:
Prostate cancer, IGRT protocol, PTV margin.

ABSTRACT

Background: External Beam Radiation Therapy (EBRT) is a curative therapy technique for prostate cancer. Since the prostate is unstable and surrounded by the bladder and rectum, precision of the target location is critical. Image Guided Radiation Therapy (IGRT) can improve treatment precision. The bladder and rectum may alter volume during IGRT, shifting the prostate's position and resulting in missed target volume doses and extra organs at risk (OARs) doses.

Objective: To assess setup error and residual error during patient positioning, as well as the current IGRT protocol efficiency, in prostate cancer patients while recommending a planning target volume (PTV) margin.

Materials and methods: The offset couch parameter of on-board imaging (OBI) and cone-beam computed tomography (CBCT) was computed to determine the error distribution, magnitude, and error difference between treatment phases. The systematic and random errors were calculated using the van Herk equation to determine the planning target volume (PTV) margin.

Results: The setup error was -0.86 to 0.25 mm, and the residual error was -0.15 to 0.32 mm. The couch displacement percentage for OBI was 29.44% to 58.89%, and for CBCT was 8.10% to 34.12%. The systematic error was 1.65 to 3.21. The random error was 1.78 to 3.29. The setup error was greatest in the longitudinal (Lng) direction, residual error was greatest in the vertical (Vrt) direction, and systematic and random error were greatest in the Vrt and lateral (Lat) direction, respectively. The PTV margin was greatest in the Vrt direction, while the Lng direction was the narrowest margin for every treatment phase.

Conclusion: The highest setup error occurs in the Lng direction for all treatment phases. For the 46 Gy and 60 Gy phases, the highest residual error is in the Vrt direction. However, in the 78 Gy phase, the error is relatively close to 0.01mm in every direction. The current IGRT protocol is effective in detecting setup and residual errors. The 78 Gy phase has the greatest PTV margin, whereas the 46 Gy phase shows the narrowest margins in all directions.

Introduction

In 2021, prostate cancer will be the fourth most frequent cancer among Thai men.[1] EBRT is one of the curative approaches for prostate cancer. The bladder and rectum are OARs for prostate cancer treatment. Position accuracy is limited by various factors, including clinical site, tumor volume, treatment technique, and immobilization device. IGRT reduces positional error by imaging the target region before administering radiation.[2] OBI and CBCT are IGRT methods for precise target volume localization that

* **Corresponding contributor.**
Author's Address: *Department of Radiological Technology, Faculty of Medical Technology, Mahidol University, Nakhon Pathom, Thailand.*
E-mail address: tawatchai.ekj@mahidol.ac.th
doi: 10.12982/JAMS.2024.036
E-ISSN: 2539-6056

may decrease the PTV margin.[3] Although CBCT takes longer than OBI, leading to increased intrafraction motion and necessitating a larger PTV margin, daily CBCT decreases errors more than non-daily CBCT.[4] According to ESTRO ACROP, the bone anatomy for prostate IGRT is insufficient since the prostate position does not correspond to the pelvic bone.[5] Fiducial markers or CT-based IGRT with soft tissue matching are recommended for detecting prostatic movements.[5] The van Herk equation is commonly used for PTV margin calculations.

At Chulabhorn Hospital, the most frequently used dose protocol for prostate cancer is 78 Gy in 39 fractions (Fx) using Volumetric Modulated Arc Therapy (VMAT). The treatment can be divided into three phases: 46Gy, 60Gy, and 78Gy. The treatment regions in each phase are as follows: 1) Prostate, seminal vesicle, and pelvic node; 2) Prostate and seminal vesicle; and 3) Prostate. For the 46 Gy and 60 Gy phases, the IGRT protocol is daily OBI and weekly CBCT, but daily OBI and daily CBCT for the 78 Gy phase. Before CT simulation and daily treatment, patients are required to maintain a full bladder to ensure accurate prostate positioning. Patients are positioned supine with hands on the chest, utilizing a cushion and foot support as immobilization devices secured to the treatment couch. On the treatment day, skin markers and in-room lasers are utilized for positioning. In this study, setup error refers to the error from the positioning, measurable using OBI, whereas residual error refers to the error that remains after OBI correction and can be measured using CBCT. After patient setup, OBI-based bone matching was performed to rectify the setup error and adjust the couch position, then CBCT-based soft tissue matching to correct the residual error and adjust the couch position before delivering radiation.

The objective of this study was to evaluate the setup error, residual error, and efficiency of the current IGRT protocol in prostate cancer. Another objective was to propose the PTV margin for the current IGRT protocol.

Materials and methods

Patients

This study was approved by Mahidol University Central Institutional Review Board (Protocol number 2022/199.2507**)** and Ethic Committee Chulabhorn Royal Academy. A total of 60 prostate cancer patients were selected from Chulabhorn Hospital's electronic medical record using a blinding procedure conducted by the participant who was not part of the study. Before the patient selection, the patient's name and hospital number were anonymized. The study included patients who underwent VMAT treatment with a dose of 78 Gy in 39 Fx following the IGRT protocol of Chulabhorn Hospital from October 2018 to January 2022. Patients for this study are treated with Varian TrueBeam LINAC (Varian Medical System, Palo Alto, CA).

Data acquisition

The offset couch parameters, representing couch values in three translation directions, were gathered from the offline review feature of the ARIA Oncology Information System (ARIA OIS) and recorded. The three translation directions were lateral (Lat: Left to Right), vertical (Vrt: Anterior to Posterior), and longitudinal (Lng: Superior to Inferior). All offset couch parameters for OBI and CBCT across fractions were collected. The offset couch parameters were vector parameters. For each patient, OBI data consisted of 39 sets, whereas CBCT data were at least 16 sets**.**

Data analysis

The 3 subprocesses were applied to each data set.

1. The offset couch parameter division

Offset couch parameters were categorized into two groups: OBI and CBCT. Each category included parameters for the three treatment phases. The total OBI data comprised 7,020 values, while the total CBCT data consisted of 3,708 values, for all treatment phases and directions.

2. Examining the setup and the residual error distribution and magnitude

The mean, standard deviation (SD), minimum, and maximum values were calculated. Box plots with a 95% confidence interval (CI) were constructed for each data set using IBM SPSS. The setup error magnitude was determined using the following equation:

$$\text{Setup error magnitude} = \sqrt{\text{SE}_{\text{Lat}}^2 + \text{SE}_{\text{Lng}}^2 + \text{SE}_{\text{Vrt}}^2}$$

where the SE_{Lat}, SE_{Lng}, and SE_{Vrt} were the lateral, longitudinal, and vertical setup errors, respectively.

3. Investigating the significant error difference between treatment phases in each direction of OBI and CBCT and observing the error direction

The Brown-Forsythe test was applied at a 95% CI to determine the error difference between treatment phases in each direction. This statistic was utilized for both OBI and CBCT. The couch displacement percentage for each direction of OBI and CBCT was calculated using Microsoft Excel to determine the error direction.

PTV margin

The PTV margin was calculated using the van Herk equation to account for setup errors observed by the current IGRT protocol. The formula was defined as 2.5 times the total SD of systematic errors plus 0.7 times the total SD of random errors.[6]

$$PTV\ margin = 2.5\Sigma + 0.7\sigma$$

The systematic error impacts all treatment fractions due to preparation error, including discrepancies in the isocenters of the LINAC, imager, and laser, as well as changes in organ shape. The population systematic error was defined as the standard deviation of all individual mean following this equation.[7]

$$\Sigma = \sqrt{\frac{1}{N-1}\sum_{i}^{N}(m_i - \bar{m})^2}$$

The random error occurs in different directions and fractions during treatment execution such as prostate motion. The population random error was defined as the root mean square of the individual SD of all patients following this equation.[8]

$$\sigma = \sqrt{\frac{1}{N}\sum_{i}^{N} s_i^2}$$

where Σ was a systemic error of all patients
σ was a random error of all patients
N was the number of patients
m_i was a systematic error of the *i*th individual patient
s_i was a random error of the *i*th individual patient
$\overline{m}$ was a mean systematic error of all patients

Results

Distribution of setup errors and magnitudes

Table 1 presented the distribution setup error in each treatment direction for every treatment phase, whereas Figure 1 showed a setup error boxplot of all phases. The median and interquartile range (IQR) of all directions and magnitudes in the three phases were similar. Although the setup error distribution of magnitude and every direction for each phase was similar, the variance of each phase differed due to large variations in sample sizes. Notably, the largest average setup error was found in the Lng direction, while the lowest was in the Lat direction for every phase.

Table 1 Distribution of setup errors in each treatment direction for each treatment phase.

Direction	Phase	Mean±SD (mm)	Maximum (mm)	Minimum (mm)
Lat	46	0.25±3.63	22.90	-13.50
	60	-0.07±3.38	11.30	-13.80
	78	0.04±3.73	14.40	-13.00
Lng	46	-0.63±2.46	14.10	-16.60
	60	-0.76±2.72	19.90	-8.40
	78	-0.86±2.73	9.20	-13.50
Vrt	46	-0.48±3.16	14.10	-11.80
	60	-0.54±3.57	10.00	-10.30
	78	-0.52±3.67	7.80	-10.40
Magnitude	46	4.69±2.81	23.89	0
	60	5.07±2.59	22.10	0
	78	5.32±2.73	16.17	0

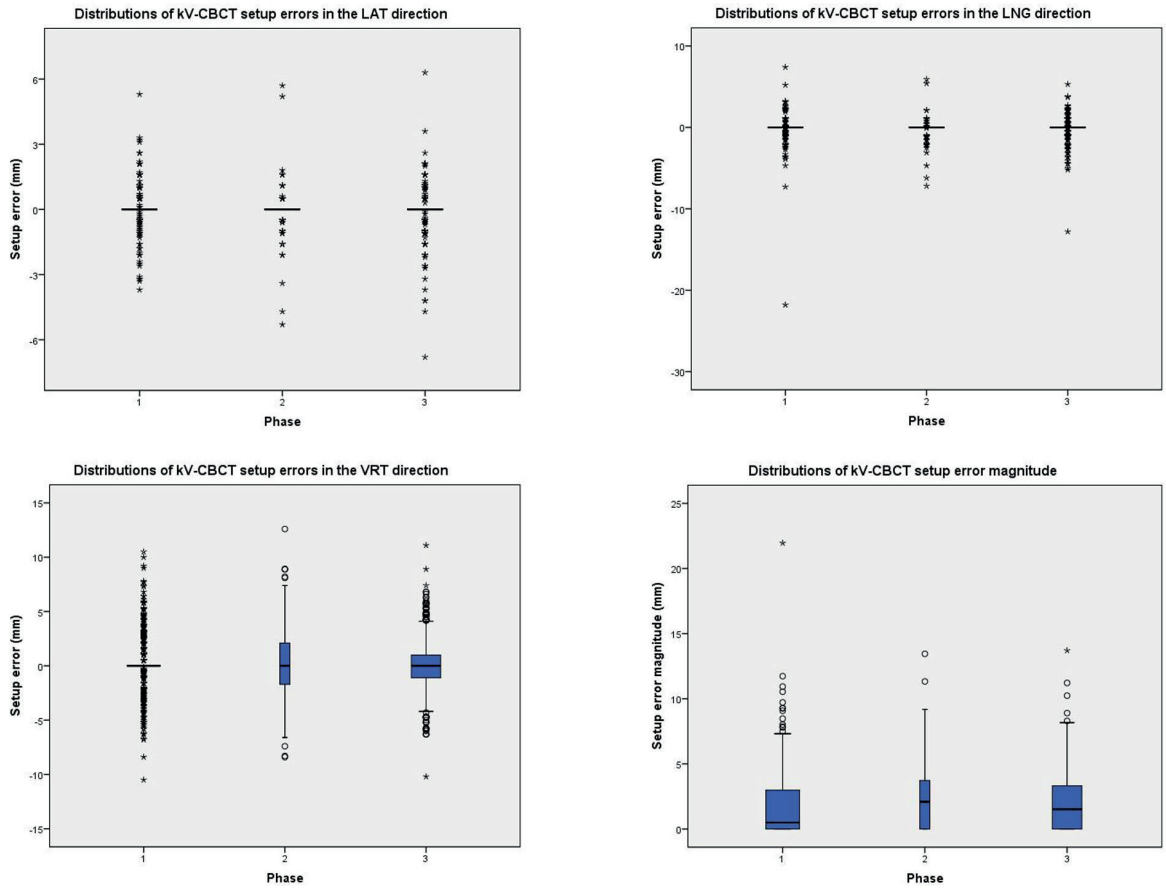

Figure 1 *Boxplot of setup error distribution of three treatment phases (Lat, Lng, Vrt, and magnitude).*

Distribution of residual errors and magnitudes

Table 2 illustrates the distribution of residual errors in each treatment direction for every treatment phase, while Figure 2 provides corresponding boxplots. The IQR for both Lat and Lng were narrow across all three phases, indicating minimal dispersion in residual error distributions. Notably, the IQR of Vrt differed among phases, with the 60 Gy phase having the widest range and the greatest dispersion in its distribution. Although the IQR of magnitudes was similar in all phases, the median for the 46 Gy phase was approximately around Q1. The distribution is right skewed for all phases. The largest average residual error was in the Vrt for the 46 Gy and 60 Gy phases but for the 78 Gy phase, the largest was in the Lat. The lowest average residual error was in the Lat for all phases.

Table 2 Distribution of residual errors in each treatment direction for each treatment phase.

Direction	Phase	Mean±SD (mm)	Maximum (mm)	Minimum (mm)
Lat	46	0.01±0.69	5.30	-3.70
	60	-0.05±1.00	5.70	-5.30
	78	-0.08±0.86	6.30	-6.80
Lng	46	-0.09±1.24	7.40	-21.80
	60	-0.15±1.19	5.90	-7.20
	78	-0.07±1.09	5.30	-12.80
Vrt	46	0.18±2.47	10.50	-10.50
	60	0.32±3.35	12.60	-8.40
	78	0.02±2.60	11.10	-10.20
Magnitude	46	1.66±2.32	21.95	0
	60	2.52±2.71	13.45	0
	78	1.98±2.19	13.71	0

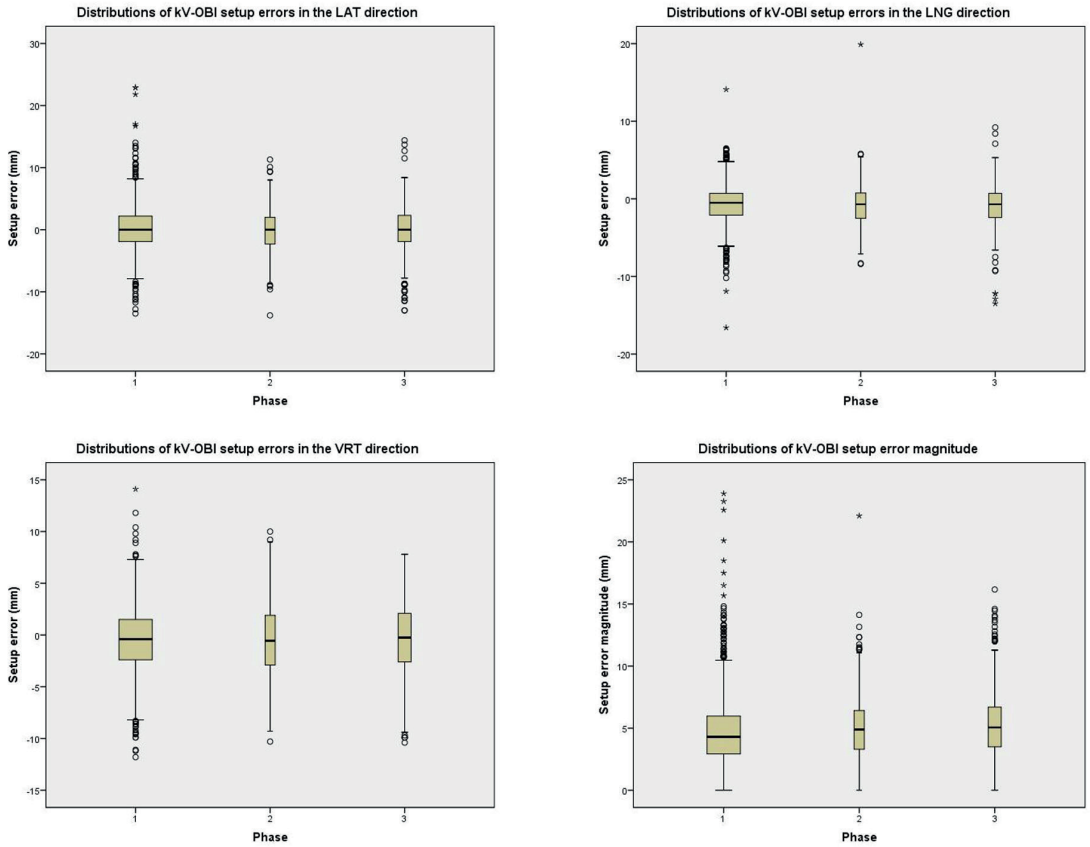

Figure 2 *Boxplot of residual error distribution of three treatment phase (Lat, Lng, Vrt, and magnitude).*

Mean difference between the three treatment phases for setup error and residual error in each direction.

The *p* values for all directions, both OBI and CBCT, were greater than 0.05. Table 3 showed that the OBI *p* values were 0.215, 0.188, and 0.926 for the Lat, Lng, and Vrt, respectively. Meanwhile, the CBCT *p* values were 0.254, 0.770, and 0.411 for the Lat, Lng, and Vrt, respectively. Notably, there were no significant differences between within-group variance and between-group variance in each phase for all directions. Table 4 showed that in the 46 Gy phase, both OBI and CBCT exhibited the highest displacement in the Vrt, and the lowest in Lng. Like the 60 Gy phase, the highest displacement was found in Vrt for both OBI and CBCT, whereas the lowest displacement of OBI was in Lat, with the CBCT in Lng. For the 78 Gy phase, the highest and lowest displacements of OBI were in Lat and Vrt, respectively, while the highest and lowest displacements of CBCT were in Vrt and Lng.

Table 3 Distribution of error difference between treatment phases in each direction of OBI and CBCT.

IGTR Protocol		*p* value
OBI	LAT-OBI	0.215
	LNG-OBI	0.188
	VRT-OBI	0.926
CBCT	LAT-CBCT	0.254
	LNG-CBCT	0.770
	VRT-CBCT	0.411

Table 4 Percentage of couch displacement of OBI and CBCT in each direction for each treatment phase.

Direction	OBI (%)			CBCT (%)		
	Phase 46 Gy	Phase 60 Gy	Phase 78 Gy	Phase 46 Gy	Phase 60 Gy	Phase 78 Gy
Left	45.32	44.76	46.85	12.15	14.12	14.46
Right	43.00	44.29	44.81	12.15	15.88	20.08
No shift	11.68	10.95	8.33	75.70	70.00	65.46
Superior	32.12	32.86	29.44	8.10	8.24	11.45
Inferior	54.82	57.38	58.89	10.39	12.94	12.25
No shift	13.05	9.76	11.67	81.51	78.82	76.31
Anterior	51.41	53.10	50.56	24.47	31.18	30.32
Posterior	38.36	37.38	37.04	24.65	34.12	28.11
No shift	10.22	9.52	12.41	50.88	34.71	41.57

Evaluation of systematic and random errors and suggested PTV margin

Table 5 displayed the computer systematic and random setup errors, along with the PTV margin for all directions and phases. The Vrt presented the greatest systematic error for all phases, while Lng presented the smallest. The random error was largest in the Lat for all phases and lowest in the Lng for the 46 Gy and 60 Gy phases, but the lowest in the 78 Gy phase was in the Lng and Vrt. For all phases, the PTV margin was greatest in the Vrt and lowest in the Lng. The PTV margin of the 78 Gy phase was the largest in all directions except the PTV margin in the Lng of the 60 Gy, which was greater than 78 Gy and 46 Gy, respectively.

Table 5 Systematic and random error and suggested PTV margins in each direction for each treatment phase.

Phase	Direction	Systematic error: Σ (mm)	Random error: σ (mm)	PTV (mm)
46 Gy	Lat	1.68	3.29	6.50
	Lng	1.65	1.88	5.43
	Vrt	2.30	2.23	7.31
60 Gy	Lat	2.21	2.77	7.46
	Lng	2.18	1.78	6.70
	Vrt	3.06	2.03	9.07
78 Gy	Lat	2.38	3.00	8.04
	Lng	2.06	1.92	6.48
	Vrt	3.21	1.91	9.36

Note: Σ: systematic error, σ: random error.

Discussion

In this study, the greatest setup error was in the Lng, followed by the Vrt and Lat in every phase. This finding contrasts with previous studies[7-10] that reported the highest setup error in Vrt. Hurkmans' study found that employing a skin marker could increase the setup error due to deviations from the respiratory, weight loss, and relaxation.[8] In our study, the incorporation of a skin marker may have contributed to the highest setup error in the Lng direction. Mayyas's study highlighted the skin marker had a large effect on the setup error in Vrt but lesser in Lat. By controlling this factor, the setup error could be reduced.[9]

Another factor influencing setup error is online image registration, but this variable is very responsive to prostate motion.[11] While 2d-kV imaging can correct the setup error, it doesn't account for prostate motion in the correction,[12] implying that the residual error was prostate motion.[13] Our study found that Vrt exhibited the highest residual error, except in the 78 Gy phase. This aligns with van Herk's findings that prostate motion was typically small, except in the Vrt direction,[14] particularly in the posterior direction.[15] Previous research found that movement of internal organs and/or targets caused variations in prostate location.[16,17] Contrary to Millender's study indicated that most of the position error was caused by setup error rather than prostate motion,[18] our findings reveal that setup errors were significantly greater than residual errors in our study.

This study observed that the setup and residual errors in the 46 Gy phase tended to have the same variation while the 60 Gy and 78 Gy phases did not, indicating that an increase in CBCT was required to correct the residual error. The current IGRT protocol for the 46 Gy and 78 Gy phases appears to be adequate; however, the protocol for the 60 Gy phase should be modified. However, when considering the PTV margin employed in treatment, the residual error in the 60 Gy phase was effectively covered by this PTV, no

adjustments were required for this protocol. Moseley's study supports the feasibility of using CBCT as the daily online IGRT for the prostate since it provided target and organ at-risk localization and enables the evaluation treatment response.[19]

In each treatment phase, the greatest PTV margin was observed in Vrt direction. Consistent with previous studies, Vrt demonstrated the greatest PTV margin.[7,9,11,20] The suggested Vrt margin ranged from 7-9 mm while the Lng margin was suggested to be 5-6 mm, corresponding to previous studies. However, this study had a larger Lat margin than previous studies due to the larger random error. Mayyas's study suggests a 10-11 mm PTV margin for skin markers and OBI before CBCT to decrease PTV by 3-5 mm.[9]

The systematic error impacts the PTV margin and is more significant than a random error since it influences the course error.[21] Daily IGRT can reduce both systematic and random error.[22,23] Daily CBCT before treatment has been shown to decrease prostate deformation with rectum and bladder control.[3] Huang's study found that daily CBCT can reduce PTV margin by 1-2 mm.[3] At Chulabhorn Hospital, the employed PTV margin for prostate cancer was 8 mm in all directions except the posterior, where it is set as 5 mm. The suggested PTV margin generally aligns within the 8 mm range, except the Vrt margin for the 60 Gy and 78 Gy phases, which exceeded the current PTV recommendation. This study was limited by the omission of the intrafraction motion error and an absence to account for the volume of the rectum and bladder.

Conclusion

The highest setup error occurs in the Lng direction for all treatment phases, with the 46 Gy phase exhibiting the least error. For the 46 Gy and 60 Gy phases, the highest residual error is in the Vrt direction. However, in the 78 Gy phase, the error is close together in every direction, with a size of no more than 0.01mm. The current IGRT protocol used for prostate cancer patients is effective in detecting setup and residual errors. The suggested PTV margin are proposed at 6.50 mm to 8.00 mm for Lat, 5.5 mm to 6.70 mm for the Lng, and 6.50 mm to 9.40 mm for Vrt direction. Notably, the 78 Gy phase has the greatest PTV margin, whereas the 46 Gy phase shows the narrowest margins in all directions.

These findings underscore the effectiveness of the current IGRT protocol and provide valuable insights for optimizing PTV margins based on specific treatment phases and directions.

Conflict of Interest

The authors declare no conflict of interest.

Funding

None

References

[1] Naravejsakul k, Pothisa T, Saenrak N. Incidence of Prostate Cancer in Physical Checkup Population with Rising of Serum Prostatic Specific Antigen. Vajira Med J. 2022; 66(5): 361-8. doi: 10.14456/vmj.2022.37.

[2] Somboon S, Malila W, Tamon S, Nueangwong W, Yeenang N, Rueansri J. Evaluation of optimal kilovoltage-cone beam technique on image quality, registration accuracy, time of imaging and relative dose for head radiotherapy: A phantom study. J Assoc Med Sci. 2022; 55(2): 10-5. doi: 10.12982/JAMS.2022.011.

[3] Huang K, Palma D, Scott D, McGregor D, Yartsev S, Louie A, *et al*. Inter- and Intrafraction Uncertainty in Prostate Bed Image-Guided Radiotherapy. Int. J. Radiat. Oncol Biol Phys. 2012; 84: 402-7. doi: 10.1016/j.ijrobp.2011.12.035.

[4] Ariyaratne H, Chesham H, Pettingell J, Alonzi R. Image-guided radiotherapy for prostate cancer with cone beam CT: dosimetric effects of imaging frequency and PTV margin. Radiother Oncol. 2016; 121(1): 103-8. doi: 10.1016/j.radonc.2016.07.018.

[5] Ghadjar P, Fiorino C, Munck Af Rosenschöld P, Pinkawa M, Zilli T, van der Heide UA. ESTRO ACROP consensus guideline on the use of image guided radiation therapy for localized prostate cancer. Radiother Oncol. 2019; 141: 5-13. doi: 10.1016/j.radonc.2019.08.027.

[6] van Herk M. Errors and margins in radiotherapy. Semin Radiat Oncol. 2004; 14(1): 52-64. doi: 10.1053/j.semradonc.2003.10.003.

[7] Hashido T, Nakasone S, Fukao M, Ota S, Inoue S. Comparison between manual and automatic image registration in image-guided radiation therapy using megavoltage cone-beam computed tomography with an imaging beam line for prostate cancer. Radiol Phys Technol. 2018; 11(4): 392-405. doi: 10.1007/s12194-018-0476-z.

[8] Hurkmans CW, Remeijer P, Lebesque JV, Mijnheer BJ. Set-up verification using portal imaging; review of current clinical practice. Radiother Oncol. 2001; 58(2): 105-20. doi: 10.1016/s0167-8140(00)00260-7.

[9] Mayyas E, Chetty IJ, Lu M, Stricker H, Pradhan D, Movsas B, *et al*. Evaluation of multiple image-based modalities for image-guided radiation therapy (IGRT) of prostate carcinoma: a prospective study. Med Phys. 2013; 40(4): 041707. doi: 10.1118/1.4794502.

[10] Ghilezan MJ, Jaffray DA, Siewerdsen JH, Van Herk M, Shetty A, Sharpe MB, *et al*. Prostate gland motion assessed with cine-magnetic resonance imaging (cine-MRI). Int J Radiat Oncol Biol Phys. 2005; 62(2): 406-17. doi: 10.1016/j.ijrobp.2003.10.017.

[11] McNair HA, Hansen VN, Parker CC, Evans PM, Norman A, Miles E, *et al*. A comparison of the use of bony anatomy and internal markers for offline verification and an evaluation of the potential benefit of online and offline verification protocols for prostate radiotherapy. Int J Radiat Oncol Biol Phys. 2008; 71(1): 41-50. doi: 10.1016/j.ijrobp.2007.09.002.

[12] Zucca S, Carau B, Solla I, Garibaldi E, Farace P, Lay G, *et al*. Prostate image-guided radiotherapy by megavolt cone-beam CT. Strahlenther Onkol. 2011; 187(8): 473-8. doi: 10.1007/s00066-011-2241-7.

[13] Poulsen PR, Muren LP, Høyer M. Residual set-up errors and margins in on-line image-guided prostate localization in radiotherapy. Radiother Oncol. 2007; 85(2): 201-6. doi: 10.1016/j.radonc.2007.08.006.

[14] van Herk M, Bruce A, Kroes AP, Shouman T, Touw A, Lebesque JV. Quantification of organ motion during conformal radiotherapy of the prostate by three dimensional image registration. Int J Radiat Oncol Biol Phys. 1995; 33(5): 1311-20. doi: 10.1016/0360-3016(95)00116-6.

[15] Ost P, De Meerleer G, De Gersem W, Impens A, De Neve W. Analysis of prostate bed motion using daily cone-beam computed tomography during postprostatectomy radiotherapy. Int J Radiat Oncol Biol Phys. 2011; 79(1): 188-94. doi: 10.1016/j.ijrobp.2009.10.029.

[16] Nakamura N, Shikama N, Takahashi O, Ito M, Hashimoto M, Uematsu M, *et al*. Variability in bladder volumes of full bladders in definitive radiotherapy for cases of localized prostate cancer. Strahlenther Onkol. 2010; 186(11): 637-42. doi: 10.1007/s00066-010-2105-6.

[17] Schallenkamp JM, Herman MG, Kruse JJ, Pisansky TM. Prostate position relative to pelvic bony anatomy based on intraprostatic gold markers and electronic portal imaging. Int J Radiat Oncol Biol Phys. 2005; 63(3): 800-11. doi: 10.1016/j.ijrobp.2005.02.022.

[18] Millender LE, Aubin M, Pouliot J, Shinohara K, Roach M, 3rd. Daily electronic portal imaging for morbidly obese men undergoing radiotherapy for localized prostate cancer. Int J Radiat Oncol Biol Phys. 2004; 59(1): 6-10. doi: 10.1016/j.ijrobp.2003.12.027.

[19] Moseley DJ, White EA, Wiltshire KL, Rosewall T, Sharpe MB, Siewerdsen JH, *et al*. Comparison of localization performance with implanted fiducial markers and cone-beam computed tomography for on-line image-guided radiotherapy of the prostate. Int J Radiat Oncol Biol Phys. 2007; 67(3): 942-53. doi: 10.1016/j.ijrobp.2006.10.039.

[20] Bylund KC, Bayouth JE, Smith MC, Hass AC, Bhatia SK, Buatti JM. Analysis of interfraction prostate motion using megavoltage cone beam computed tomography. Int J Radiat Oncol Biol Phys. 2008; 72(3): 949-56. doi: 10.1016/j.ijrobp.2008.07.002.

[21] van Herk M, Remeijer P, Rasch C, Lebesque JV. The probability of correct target dosage: dose-population histograms for deriving treatment margins in radiotherapy. Int J Radiat Oncol Biol Phys. 2000; 47(4): 1121-35. doi: 10.1016/s0360-3016(00)00518-6.

[22] Ding GX, Coffey CW. Radiation dose from kilovoltage cone beam computed tomography in an image-guided radiotherapy procedure. Int J Radiat Oncol Biol Phys. 2009; 73(2): 610-7. doi: 10.1016/j.ijrobp.2008.10.006.

[23] Wang G, Wang WL, Liu YQ, Dong HM, Hu YX. Positioning error and expanding margins of planning target volume with kilovoltage cone beam computed tomography for prostate cancer radiotherapy. Onco Targets Ther. 2018; 11: 1981-8. doi: 10.2147/ott.S152915.